RAB-10-GTPase–mediated regulation of endosomal phosphatidylinositol-4,5-bisphosphate

Anbing Shi[a,b], Ou Liu[a], Sabine Koenig[c], Riju Banerjee[a], Carlos Chih-Hsiung Chen[a,d], Stefan Eimer[c,e], and Barth D. Grant[a,1]

[a]Department of Molecular Biology and Biochemistry and [d]The Waksman Institute, Rutgers University, Piscataway, NJ 08854; [b]Department of Biology, Stanford University, Stanford, CA 94305; [e]Centre for Biological Signalling Studies (BIOSS), Albert-Ludwigs-Universitaet Freiburg, 79117 Freiburg, Germany; and [c]European Neuroscience Institute, 37077 Göttingen, Germany

Edited by Peter S. McPherson, Montreal Neurological Institute, McGill University, Montreal, Canada, and accepted by the Editorial Board July 10, 2012 (received for review March 30, 2012)

Caenorhabditis elegans **RAB-10 and mammalian Rab10 are key regulators of endocytic recycling, especially in the basolateral recycling pathways of polarized epithelial cells. To understand better how RAB-10 contributes to recycling endosome function, we sought to identify RAB-10 effectors. One RAB-10-binding partner that we identified, CNT-1, is the only *C. elegans* homolog of the mammalian Arf6 GTPase-activating proteins ACAP1 and ACAP2. Arf6 is known to regulate endosome-to-plasma membrane transport, in part through activation of type I phophatidylinositol-4-phosphate 5 kinase. Here we show that CNT-1 binds to RAB-10 through its C-terminal ankyrin repeats and colocalizes with RAB-10 and ARF-6 on recycling endosomes in vivo. Furthermore, we find that RAB-10 is required for the recruitment of CNT-1 to endosomal membranes in the intestinal epithelium. Consistent with negative regulation of ARF-6 by RAB-10 and CNT-1, we found overaccumulation of endosomal phosphatidylinositol-4,5-bisphosphate [PI(4,5)P2] in *cnt-1* and *rab-10* mutants and reduced endosomal PI(4,5)P2 levels in *arf-6* mutants. These mutants produced similar effects on endosomal recruitment of the PI(4,5)P2-dependent membrane-bending proteins RME-1/Ehd and SDPN-1/Syndapin/Pacsin and resulted in endosomal trapping of specific recycling cargo. Our studies identify a RAB-10–to–ARF-6 regulatory loop required to regulate endosomal PI(4,5)P2, a key phosphoinositide in membrane traffic.**

membrane lipid | clathrin

Endocytic recycling is essential for counterbalancing endocytosis and is important for a host of higher-order processes such as cytokinesis, cell migration, maintenance of polarized cell membrane domains, and synaptic plasticity (1). Small GTPases of the Rab and Arf families have long been known to be key regulators of membrane traffic, and certain members of these families function specifically in endocytic recycling (2–7).

Previous studies in our laboratory indicated that RAB-10 is required for the basolateral recycling of clathrin-independent cargo such as hTAC-GFP in the *Caenorhabditis elegans* intestine (5, 8). In the *C. elegans* nervous system, RAB-10 also is required for the recycling of AMPA-type glutamate receptors in postsynaptic membranes (9). Accumulating evidence suggests that RAB-10 functions upstream of RME-1/Ehd, a peripheral membrane protein involved in recycling endosome tubulation and probably endosome fission (5, 8, 10). In polarized MDCK cells Rab10 also functions in basolateral recycling (11). Additionally, in mammalian adipocytes Rab10 was reported to regulate the insulin-dependent recycling of Glut4 glucose transporters (12). *C. elegans* intestinal RAB-10–labeled endosomes often are positive for RAB-5, RAB-8, and RAB-11 (5). Such endosomes are likely to be counterparts of the Rab10-positive common recycling endosome (CRE) in MDCK cells. CREs are thought to receive, sort, and recycle cargo received from both the apical and basolateral plasma membrane domains (11).

Of the Arfs, Arf6 is most closely associated with endocytic recycling regulation. The requirement for Arf6 in endosomal recycling was documented first in CHO cells, in which the expression of the dominant-negative Arf6(T27N) blocked the recycling of both clathrin-dependent and -independent cargos (13). In HeLa cells expression of GTP hydrolysis-defective Arf6(Q67L) caused phosphatidylinositol-4,5-bisphosphate [PI(4,5)P2] and actin accumulation on endosomes, sequestering clathrin-independent cargo proteins but not clathrin-dependent cargo transferrin receptors (TfR) in the abnormal endosomes (14). Although reports vary, siRNA-mediated knockdown of Arf6 or expression of dominant-negative Arf6(T27N) in HeLa cells generally affects the recycling of integral plasma membrane proteins that lack cytoplasmic clathrin adaptor-sorting sequences, such as TAC, MHC class I protein (MHCI), GPI-anchored proteins, and certain cell-adhesion molecules (15–17). Recycling of these cargos occurs through Arf6-positive tubules that emanate from the juxtanuclear endocytic recycling compartment (16). These tubules may represent a recycling route separate from that taken by other recycling cargo such as TfR (16).

Arf6 regulates endocytic recycling, at least in part, through activation of enzymes that modify membrane lipids (18). In tissue culture cells, Arf6 localizes with and activates type I phophatidylinositol-4-phosphate 5 kinase (PIP5KI) (19). PIP5KI is responsible for phosphorylating PI(4)P to generate PI(4,5)P2, a major plasma membrane and recycling endosome phosphoinositide that is required to recruit and activate many peripheral membrane proteins that mediate membrane traffic and actin polymerization (19, 20).

In our effort to identify interacting partners of RAB-10, we recovered CNT-1, the *C. elegans* homolog of mammalian ACAP1/2 [for Arf GAP, with Coil, ankyrin (ANK) repeat, pleckstrin homology (PH) domain]. ACAP1/2 (Centaurin beta 1/2) belongs to the AZAP-type of Arf GTPase-activating proteins (GAPs) (21). Biochemical studies have suggested that ACAP1 and ACAP2 preferentially activate the GTPase activity of Arf6 over other Arfs and that the ACAPs are activated by PI(4,5)P2 binding (22). Furthermore, PIP5KI, which is positively regulated by Arf6(GTP), seems to function with ACAP1 to enhance endosomal tubulation (23). Here we demonstrate that CNT-1 functions as a RAB-10 effector to regulate ARF-6–dependent endocytic recycling. Interestingly, either the loss of CNT-1 or the overexpression

Author contributions: A.S., S.E., and B.D.G. designed research; A.S., O.L., S.K., R.B., and C.C.-H.C. performed research; A.S., O.L., and S.K. contributed new reagents/analytic tools; A.S., O.L., S.K., S.E., and B.D.G. analyzed data; and A.S. and B.D.G. wrote the paper.

The authors declare no conflict of interest.

This article is a PNAS Direct Submission. P.S.M. is a guest editor invited by the Editorial Board.

[1]To whom correspondence should be addressed. E-mail: grant@biology.rutgers.edu.

See Author Summary on page 13892 (volume 109, number 35).

This article contains supporting information online at www.pnas.org/lookup/suppl/doi:10.1073/pnas.1205278109/-/DCSupplemental.

of CNT-1 results in the endosomal accumulation of the model ARF-6–dependent cargo protein hTAC-GFP. Our data provide evidence of a RAB-to-ARF regulatory loop influencing endosomal PI(4,5)P2 levels and the recruitment of endosomal membrane-bending proteins.

Results

C-Terminal ANK Repeat Sequence of CNT-1 Is a Rab-Interacting Domain. To understand better how RAB-10 controls endocytic recycling, we sought to identify RAB-10 effectors via a yeast two-hybrid screen using a predicted constitutively active (GTPase-defective) form of RAB-10, Q68L, as bait (8). Of the 70 clones that tested positive for interaction with RAB-10(Q68L) in Leu2 and β-galactosidase expression assays, two clones were identified that encoded full-length CNT-1 (*Materials and Methods*). No interaction was detected between CNT-1 and a predicted GDP-bound mutant form RAB-10, T23N, or wild-type RAB-10 (Fig. 1*A* and Fig. S1*A*), suggesting that CNT-1 preferentially interacts with the active form of RAB-10.

CNT-1 was a particularly interesting candidate interactor for RAB-10, because it is the only *C. elegans* homolog of mammalian ACAP1 and ACAP2, GAPs for the class III Arf-GTPase Arf6. Binding of RAB-10 to CNT-1 suggested a link between the activities of RAB-10 and ARF-6 during endocytic recycling. Like Arf6, mammalian ACAP1 is required for the recycling of endocytic cargo proteins and is enriched on recycling endosome tubules that contain Arf6, PIP5KI, and PI(4,5)P2 (22, 23). Like ACAP1 and ACAP2, CNT-1 contains tandem predicted lipid-binding domains [an N-terminal bin-amphiphysin-rvs (BAR) domain followed by a PH domain] in addition to a central ARF-GAP domain and a C-terminal ANK-repeat domain (23).

To determine the region of CNT-1 that interacts with RAB-10, we tested various truncations of CNT-1 in the two-hybrid assay with RAB-10(Q68L). These experiments delimited the RAB-10 binding site within CNT-1, showing that the segment containing the C-terminal ANK repeat (amino acids 656–826) is necessary and sufficient to mediate the interaction with RAB-10 (Fig. 1 *B*–*D*). To determine the specificity of the CNT-1 interaction with

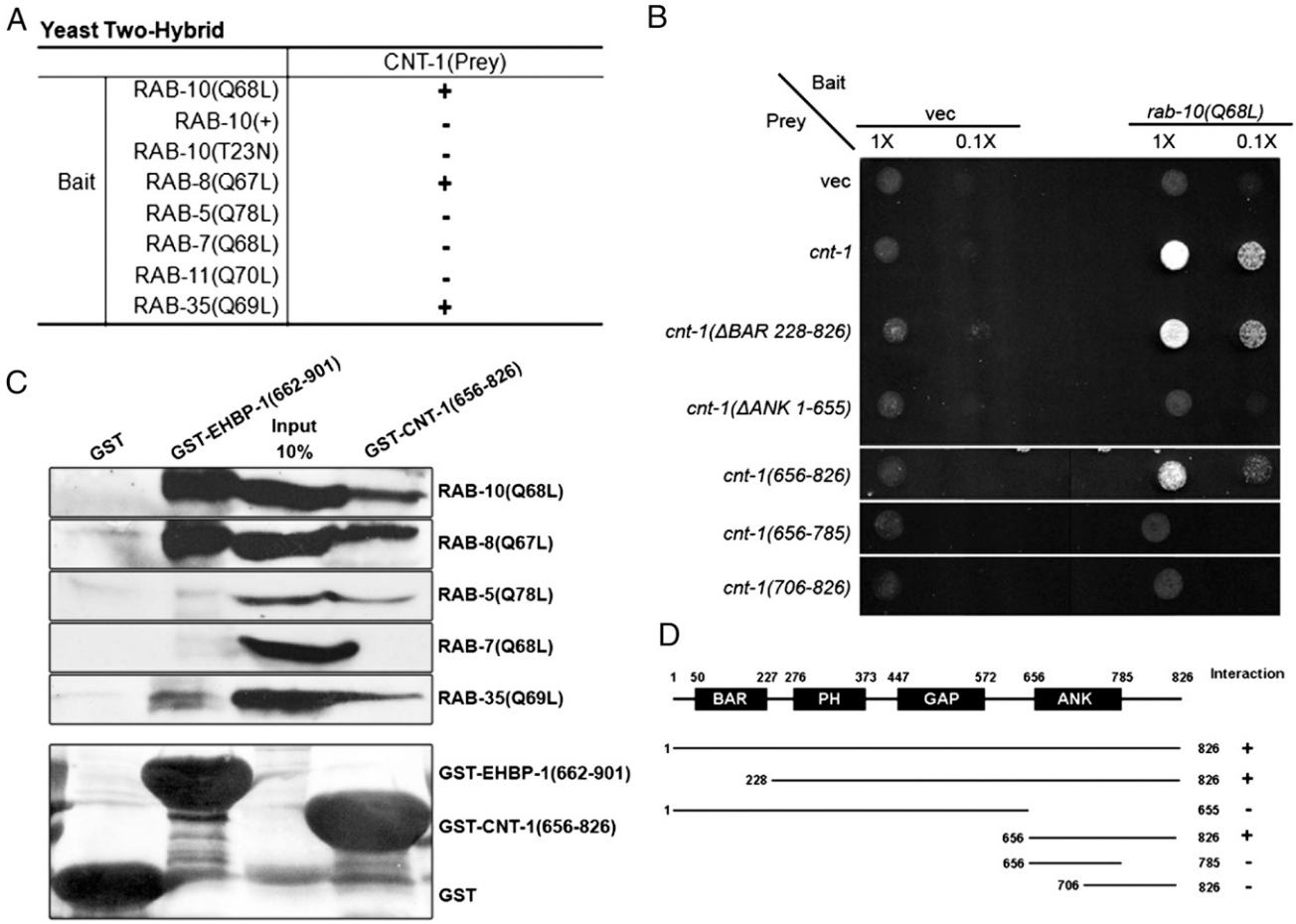

Fig. 1. CNT-1 interacts physically with RAB-10. (*A*) Binding specificity of CNT-1 with RAB-8, RAB-10, and RAB-35. Using full-length CNT-1 as prey, Rabs with reported endosomal trafficking involvement, including active RAB-5(Q78L), RAB-7(Q68L), RAB-8(Q67L), RAB-10(Q68L), RAB-10(+), RAB-10(T23N), RAB-11(Q70L), and RAB-35(Q69L), were used as bait in the yeast two-hybrid assays. (*B*) The interaction between CNT-1 and RAB-10(Q68L) requires the CNT-1 segment containing the C-terminal ANK repeat. RAB-10(Q68L) was expressed in a yeast reporter strain as a fusion with the DNA-binding domain of LexA (bait). Truncated CNT-1 forms were expressed in the same yeast cells as fusions with the B42 transcriptional activation domain (prey). Interaction between bait and prey was assayed by complementation of leucine auxotrophy (LEU2 growth assay). Colonies were diluted in liquid and spotted on solid growth medium directly or after further dilution. (*C*) Glutathione beads loaded with recombinant GST, GST-EHBP-1 (amino acids 662–901), and GST-CNT-1 (amino acids 656–826) were incubated with in vitro-expressed HA-tagged RAB-5(Q78L), RAB-7(Q68L), RAB-8(Q67L), RAB-10(Q68L), and RAB-35(Q69L) and then were washed to remove unbound proteins. (*Lower*) Eluted proteins were separated on SDS/PAGE and stained with Ponceau S to detect GST fusion proteins. (*Upper*) Bound proteins were eluted and analyzed by Western blot using anti-HA. Input lanes contain in vitro-expressed HA-tagged RABs used in the binding assays (10%). (*D*) Schematic representations of CNT-1 domains and the truncated fragments used in the Y2H analysis. Protein domains are displayed as dark boxes above the protein sequences (shown as dark lines) used in the study. Amino acid numbers are indicated.

RAB-10, we assayed other endocytic Rab-GTPases. RAB-5 (Q78L), RAB-7(Q68L), and RAB-11(Q70L) failed to interact with CNT-1, but RAB-8(Q67L) and RAB-35(Q69L) displayed a robust interaction with CNT-1 in this assay, interacting with the same ANK repeat-containing segment (amino acids 656–826) that interacts with RAB-10 (Fig. 1*A* and Fig. S1 *B* and *C*). RAB-8 is the closest paralog of RAB-10 in *C. elegans* and is redundant with RAB-10 in some nonpolarized cell types (8). Like RAB-10 and RAB-8, RAB-35 is an important recycling regulator in *C. elegans* and mammals (7, 24). We also tested these binding interactions using a GST-pulldown approach, using GST-only as a negative control and EHBP-1, a RAB-10 effector that we previously identified, as a positive control (Fig. 1*C*). This experiment confirmed the interaction of CNT-1(ANK) with the active forms of RAB-10, RAB-8, and RAB-35, whereas EHBP-1 interacted only with RAB-10 and RAB-8 (Fig. 1*C*). Interestingly, binding of the CNT-1 ANK domain to RAB-5(Q78L) also was detected in our pulldown assay but was not detected in the two-hybrid assay (Fig. 1*C*). Taken together, these results indicate that the C-terminal ANK repeats of CNT-1 provide a binding surface with the potential to interact with a subgroup of Rabs associated with endocytic recycling.

CNT-1 Is Enriched on Endosomes. To determine if CNT-1 is associated with the same organelles as these recycling Rabs in vivo, we assayed the subcellular localization of functional mCherry (MC)-tagged CNT-1 fusion proteins expressed specifically in the intestinal epithelial cells (Fig. S2 *H–J*), a tissue with well-established markers for endomembrane compartments (5, 8, 25). CNT-1 localized strongly to intracellular puncta that were similar in size and shape to endosomes (see Fig. 3*A*). CNT-1 also displayed enrichment on or near the basolateral and apical plasma membranes (Fig. 2*A′*). Consistent with our binding data, we observed extensive colocalization of CNT-1-MC with endosomes labeled by GFP-RAB-10, GFP-RAB-8, and GFP-RAB-35 (Fig. 2 *A–B″* and Fig. S2 *A–A″*). In these cells RAB-10 is required for basolateral recycling, and RAB-8 has been implicated in apical transport (5, 26). RAB-10 and RAB-8 colocalize extensively on endosomes in this tissue, suggesting that this organelle sorts basolateral and apical cargos (5, 8). This notion is consistent with the localization of mammalian Rab10 to the CRE, an organelle that receives and sorts basolateral and apical cargos, in polarized MDCK cells (11, 27). RAB-35 had not been studied in the intestine previously, but we had previously shown that RAB-35 is expressed ubiquitously and is required for receptor recycling in the *C. elegans* oocyte cells (7). These results are consistent with CNT-1 acting as an effector for Rab-GTPases during endocytic recycling.

Like RAB-10, CNT-1-MC showed partial colocalization with the early endosome marker GFP-RAB-5 and showed little overlap with the late-acting recycling endosome protein GFP-RME-1 (Fig. 2 *C–C″* and Fig. S2 *B–B″*). Likewise, little overlap was observed between CNT-1-MC and GFP-ALX-1 (Fig. S2 *C–C″*), which labels both RME-1–positive basolateral recycling endosomes and ESCRT-enriched multivesicular endosomes (MVEs) (25). The Golgi ministack marker MANS-GFP generally was found closely juxtaposed to CNT-1-MC–labeled endosomes but with little direct overlap (Fig. S2 *D–D″*), again similar to the localization we previously described for RAB-10 (5, 8). Collectively, our results demonstrate that CNT-1 is enriched on recycling endosomes, where it could potentially interact with RAB-10, RAB-8, and/or RAB-35 to regulate endosome-to-plasma membrane transport of cargo derived from the plasma membrane and/or the Golgi.

RAB-10 Is Required for CNT-1 Endosomal Recruitment. Many of the proteins that bind to GTP-bound Rabs are effector proteins, and such effectors often are localized and/or activated by interaction with their cognate Rab(s) (28). To determine whether CNT-1 displays such a relationship with any of the Rabs with which it can bind, we assayed for changes in the localization of CNT-1-GFP in the relevant *rab*-mutant backgrounds. We found a dramatic redistribution of CNT-1-GFP in *rab-10(q373)* mutants. CNT-1-GFP appeared very diffusive in *rab-10* mutants, displaying an almost complete loss of CNT-1-GFP endosomal localization (Fig. 3 *A*, *C*, and *E*). Loss of RAB-8 had a minor effect on CNT-1-GFP localization, with an average reduction in puncta intensity of about 20% in *rab-8(tm2526)* mutants (Fig. 3 *D* and *E*). CNT-1-GFP localization and puncta intensity was unaffected in *rab-35(b1013)* mutants (Fig. S2 *E–G*). The intensity of CNT-1-GFP labeling of endosomes was increased mildly in *rme-1(b1045)* mutants that are defective in a later step in the basolateral recycling pathway (Fig. 3 *B* and *E*). These results indicate that, at least in this tissue, RAB-10 is the dominant Rab GTPase recruiting CNT-1 to endosomes.

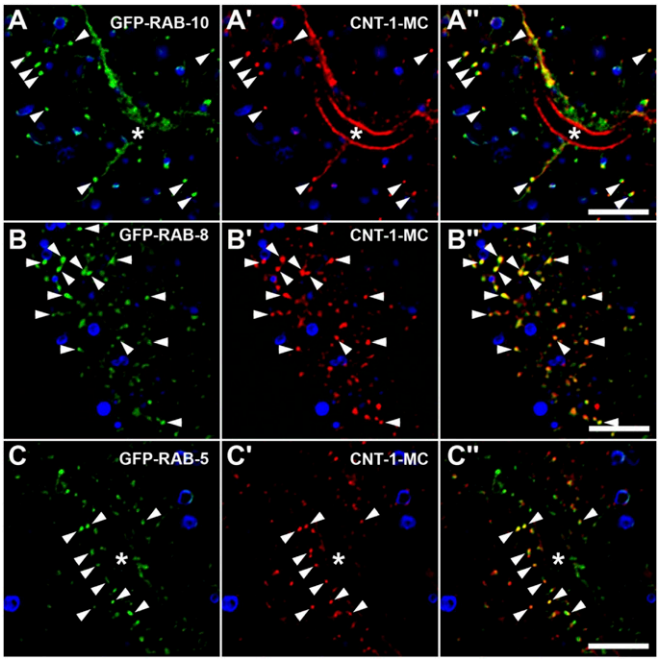

Fig. 2. CNT-1 colocalizes with RAB-10 on endosomes. (*A–C″*) Colocalization images are from deconvolved 3D image stacks acquired in intact living animals expressing GFP- and mCherry-tagged proteins specifically in intestinal epithelial cells. (*A–A″*) CNT-1-MC colocalizes with GFP-RAB-10. Arrowheads indicate endosomes labeled by both CNT-1-MC and GFP-RAB-10. (*B–B″*) CNT-1-MC colocalizes with GFP-RAB-8 on endosomal structures. Arrowheads indicate endosomes labeled by both CNT-1-MC and GFP-RAB-8. (*C–C″*) CNT-1-MC partially colocalizes with GFP-RAB-5 on endosomal structures. Arrowheads indicate endosomes labeled by both CNT-1-MC and GFP-RAB-5. In each image autofluorescent lysosome-like organelles can be seen in all three channels; the strongest signal is in blue. GFP appears only in the green channel, and mCherry appears only in the red channel. Signals observed in the green or red channels that do not overlap with signals in the blue channel are considered bone fide GFP or RFP signals, respectively. Asterisks in *A* and *C* indicate intestinal lumen. (Scale bar: 10 μm.)

CNT-1 and RAB-10 Colocalize with ARF-6 in the Basolateral Recycling Pathway. As a first test of a functional connection of CNT-1 and RAB-10 with ARF-6, we assayed for colocalization of each protein with ARF-6 in the *C. elegans* intestine. We found that a functional ARF-6-GFP fusion protein labels punctate and tubular membrane structures in the intestinal cells and overlaps extensively with CNT-1-MC on endosomes (Fig. S3 *G–G″*). Consistent with the potential connection of ARF-6 and RAB-10, we found that ARF-6-GFP also colocalized well with MC-RAB-10 on recycling endosomes (Fig. S3 *H–H″*). To a lesser extent ARF-6-GFP also labeled the RME-1–positive recycling endo-

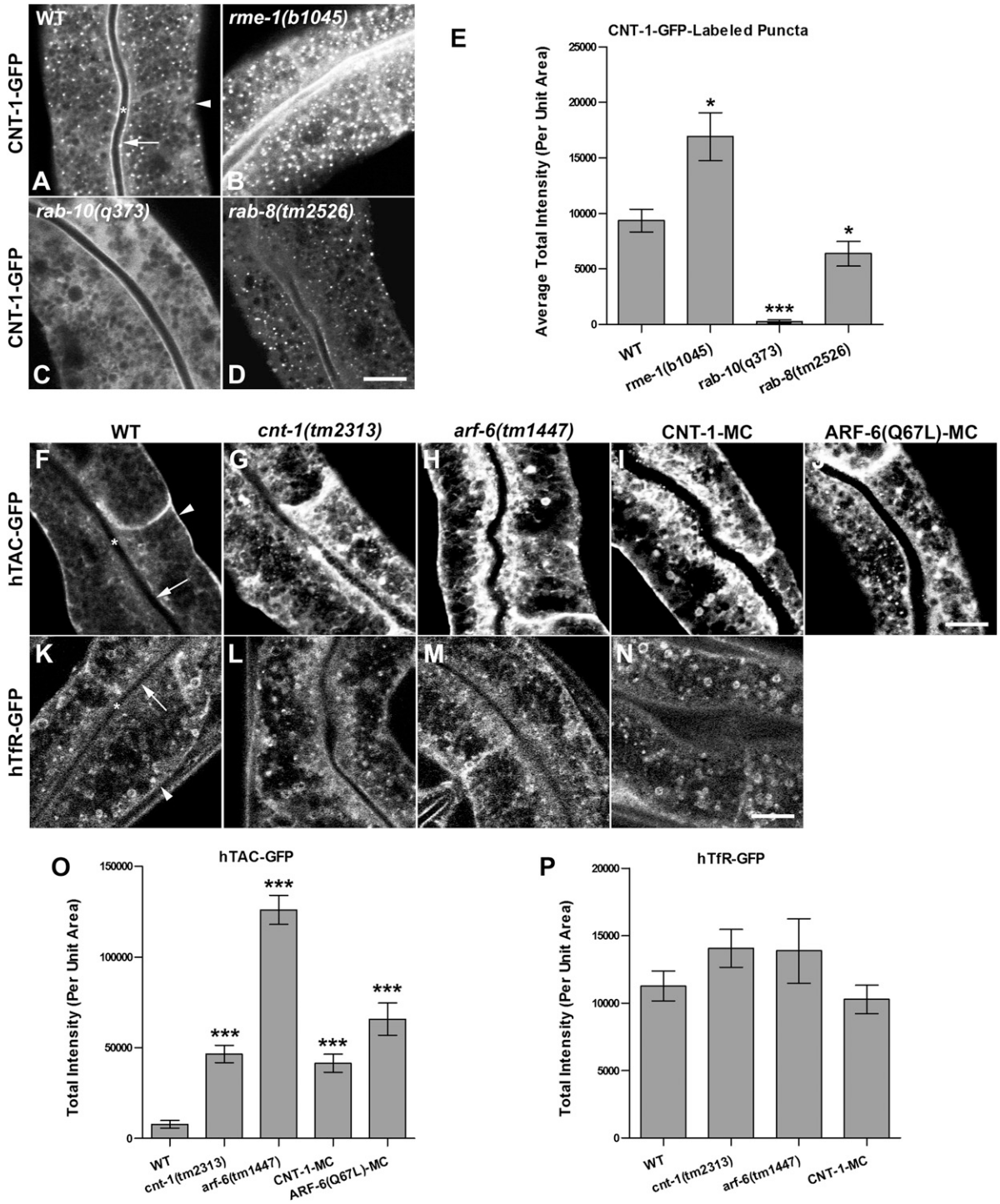

Fig. 3. (*A*–*E*) CNT-1 loses its endosomal association in *rab-10* mutants. Representative confocal images are shown for CNT-1-GFP in wild-type animals (*A*) and in *rme-1(b1045)* (*B*), *rab-10(q373)* (*C*), and *rab-8(tm2526)* (*D*) mutants. Average total intensity of CNT-1-GFP per unit area is quantified in *E*. (*C* and *E*) Loss of functional RAB-10 disrupts CNT-1 endosomal association. (*B* and *E*) Depletion of RME-1 increases the accumulation of CNT-1-GFP–positive puncta with an approximately twofold average increase in total intensity per unit area. (*D* and *E*) Loss of RAB-8 has a minor effect on CNT-1-GFP localization, displaying an average reduction in puncta intensity of about 20% in *rab-8(tm2526)* mutants. (*F*–*P*) Loss of CNT-1 induces cargo recycling defects in the *C. elegans* intestine. Confocal images of the worm intestine expressing GFP-tagged cargo proteins that recycle via the recycling endosome, the human transferrin receptor (hTfR-GFP), and the IL-2 receptor α chain (hTAC-GFP) in wild-type and in *cnt*-1(tm2313)– and *arf-6(tm1447)*–mutant animals. Compared with wild-type animals (*F*), hTAC-GFP accumulates significantly in the intestinal cytosolic endosomal structures (~sixfold increase) in *cnt-1(tm2313)* mutants (*G* and *O*) and increases in *arf-6(tm1447)* mutants (*H* and *O*) by ~50-fold. hTfR-GFP was not affected in *cnt-1(tm2313)* (*L* and *P*) and *arf-6(tm1447)* mutants (*M* and *P*). Intracellular hTAC-GFP accumulates in intestinal cells with overexpressed CNT-1 (*I* and *O*). Expression of the *C. elegans* ARF-6 GTPase–defective form ARF-6 (Q67L) (*J* and *O*) greatly impaired hTAC-GFP localization and caused trapping of hTAC-GFP in endosomes. In *A*, *F*, and *K*, asterisks indicate intestinal lumen, arrows indicate apical membrane, and arrowheads indicate basolateral membrane. Error bars in *E*, *O*, and *P* represent SEM. $n = 18$; three different regions of the intestine (defined by a 100 × 100 pixel box positioned at random) were sampled in six animals of each genotype. $^{*}P < 0.01$, $^{***}P < 0.001$, one-tailed Student's *t* test. (Scale bar: 10 μm.)

somes close to the basolateral plasma membrane, further indicating that ARF-6 is present on endosomes associated with basolateral recycling (Fig. S3 *I–I″*).

Neither RAB-10 nor RME-1 function was required for ARF-6 endosomal recruitment. ARF-6-GFP remained localized to endosomal puncta and tubules in *rab-10* and *rme-1* mutants and also labeled the limiting membrane of the grossly enlarged early and recycling endosomes that accumulate in *rab-10* and *rme-1* mutants, respectively (Fig. S3 *B*, *C*, and *E*). Notably, we observed an overaccumulation of ARF-6-GFP–positive basolateral tubules and punctae in *cnt-1(tm2313)* mutants, suggesting in vivo relevance for CNT-1 in ARF-6 function (Fig. S3 *D* and *E*). GFP-RAB-10 intensity also increased in *cnt-1* mutants (see Fig. S5*B*). We did not find any effect of *cnt-1* mutants on the late endosomal markers GFP-RAB-7 and LMP-1-GFP or on the MVE/multivesicular body (MVB) marker HGRS-1/Hrs (see Fig. S5 *E*, *H*, and *K*). The *cnt-1(tm2313)* mutant used in this analysis is a 344-base deletion and single-base insertion in the ninth exon of *cnt-1*. This *cnt-1* mutation is predicted to introduce a frame-shift and stop codon soon after the deletion, removing the majority of the predicted CNT-1 GAP domain and all of the predicted ANK repeats (Δ472–826).

We also tested the importance of ARF-6 in the localization of CNT-1 and RAB-10. The *arf-6* mutant *tm1447* used in these studies deletes nearly the entire *arf-6* gene and does not produce any ARF-6 protein as judged by anti–ARF-6 Western blot (Fig. S3*F*). Neither CNT-1 nor RAB-10 required ARF-6 for endosomal localization. Instead, we noted that both CNT-1-GFP and GFP-RAB-10 labeling of endosomes increased in intensity in *arf-6(tm1447)* mutants (Figs. S4 *B* and *C* and S5 *C* and *M*). Further analysis showed that CNT-1-RFP and GFP-RAB-10 remain colocalized in *arf-6* mutants (Fig. S4 *D–D″*). These results may reflect a block in the recycling pathway downstream of RAB-10 in *arf-6* (and *cnt-1*) mutants. We did not find any effect of *arf-6* mutants on the late endosomal markers GFP-RAB-7 and LMP-1-GFP or on the MVE/MVB marker HGRS-1/Hrs (Fig. S5 *F*, *I*, and *L*). In summary, these studies establish that CNT-1, RAB-10, and ARF-6 overlap in localization on endosomes of the basolateral recycling pathway and that the loss of any of the three proteins affects the morphology of endosomes labeled by the others.

Loss of CNT-1 Affects ARF-6–Dependent Cargo. To test further the functional relationship of CNT-1 and ARF-6, we assayed deletion alleles of *cnt-1* and *arf-6* for effects on the well-defined recycling cargo proteins hTAC-GFP and human TfR (hTfR)-GFP (5, 25). In HeLa cells Arf6 preferentially affects recycling of CIE cargo such as TAC but has very little effect on clathrin-dependent endocytosis cargo TfR (15, 16). In our previous work we showed that loss of RAB-10 preferentially traps hTAC-GFP in the endosomal system but has very little effect on hTfR-GFP (5, 8). Consistent with its cargo specificity in mammals, we observed a dramatic intracellular accumulation of hTAC-GFP in the intestinal cells of *arf-6(tm1447)* mutants (Fig. 3 *H* and *O*), but no such effect was found for hTfR-GFP (Fig. 3 *M* and *P*). Most of the overaccumulated hTAC-GFP in *arf-6* mutants colocalized with the recycling endosome marker EHBP-1-RFP (Fig. S6 *A–A″*) (8). We observed a similar intracellular accumulation of hTAC-GFP in intestinal cells overexpressing CNT-1, a perturbation that would be expected to inactivate ARF-6 and mimic the *arf-6* loss-of-function phenotype (Fig. 3 *I* and *O*).

A full Arf6 GTPase cycle is thought to be important for the efficient recycling of CIE cargo (15, 18). In HeLa cells MHCI and TAC recycling also is impaired upon expression of the GTP hydrolysis-defective mutant ARF-6(Q67L) (16). Likewise, we found that expression of *C. elegans* ARF-6(Q67L) caused apparent trapping of hTAC-GFP in endosomes (Fig. 3 *J* and *O*). Because CNT-1 is an ARF-6 GAP, loss of CNT-1 would be expected to result in elevated levels of ARF-6(GTP) and impaired recycling of hTAC. Indeed we observed endosomal accumulation of hTAC-GFP in *cnt-1(tm2313)* mutants, and the accumulated hTAC-GFP colocalized with recycling endosome marker EHBP-1-RFP (Fig. 3 *G* and *O* and Fig. S6 *B–B″*) (8). Our results provide in vivo evidence of the importance of the ARF-6 GTPase cycle in the regulation of CIE cargo recycling in *C. elegans* and indicate a clear requirement for CNT-1 in this process.

Loss of RAB-10 Leads to Increased Accumulation of PI(4,5)P2. Because PIP5KI is an important Arf6 effector, and CNT-1 is expected to inactivate ARF-6, loss of CNT-1 or RAB-10 would be expected to increase PI(4,5)P2 levels, and loss of ARF-6 would be expected to reduce PI(4,5)P2 levels (18–20). We sought to test these predictions by assaying the subcellular distribution of PI(4,5)P2 in the *C. elegans* intestinal cells, using the PI(4,5)P2 biosensor PH(PLCδ)-GFP, which contains the PI(4,5)P2-specific binding PH domain of the rat phospholipase Cδ (29). As controls, we also assayed the subcellular localization of PI(3)P and PI(3,4,5)P3 using the biosensors GFP-2xFYVE(HRS) and PH(Akt)-GFP. In wild-type animals we noted that PH(PLCδ)-GFP labels the apical and basolateral plasma membrane as well as internal puncta and tubules (Fig. 4*A* and Fig. S7 *J* and *J′*). The intracellular puncta and tubules labeled with PH(PLCδ)-GFP colocalize extensively with functional ARF-6-MC, identifying them as endosomes along the basolateral recycling pathway (Figs. S2*M* and S7 *A–A″*). Extensive overlap also can be observed on the apical and lateral plasma membrane (Fig. S7 *B–B″*). The PI(3)P marker GFP-2xFYVE(HRS) localized relatively diffusely in the intestinal cells, with only rare visible puncta (Fig. S7*C*). The PI(3,4,5)P3 marker PH(Akt)-GFP labeled rare cytoplasmic puncta and the apical and basolateral plasma membranes, although neither plasma membrane was labeled as strongly by the PI(3,4,5)P3 marker as by the PI(4,5)P2 marker (Fig. S7*F*).

In *arf-6*–null mutant animals we observed a significant decrease in PH(PLCδ)-GFP labeling of endosomal puncta and tubules (Fig. 4 *C* and *D*). These findings indicate that ARF-6 is important for regulating endosomal PI(4,5)P2 levels. Conversely, we found that in *cnt-1* and *rab-10* mutants PH(PLCδ)-GFP labeling on the basolateral endosomal puncta and tubules was increased, as would be expected if ARF-6 activity is increased in these mutant backgrounds (Fig. 4 *B*, *D*, *F*, and *G*). However, the apparent increase of PI(4,5)P2 labeling was greater in *rab-10* mutants than in *cnt-1* mutants, suggesting that only part of the effect of RAB-10 on PI(4,5)P2 could be explained by failure in recruiting CNT-1 to membranes. We also detected an increase in PH(PLCδ)-GFP labeling in the intestine of *rab-8*–mutant animals (Fig. S7 *L–N*), consistent with the mildly reduced endosomal recruitment of CNT-1 observed in *rab-8* mutants (Fig. 3 *D* and *E*). In this case, however, the increased PI(4,5)P2 biosensor labeling was near the apical membranes, consistent with a proposed role for RAB-8 in apical transport (26). As shown in Fig. S7, the levels of PI(3)P (labeled by GFP-2xFYVE) and PI(3,4,5)P3 (labeled by PH(Akt)-GFP) appeared unperturbed in *cnt-1* and *arf-6* mutants (Fig. S7 *C–I*), indicating the specificity of the effects. Interestingly, the intensity of PH(PLCδ)-GFP labeling was not detectably altered in *rme-1* mutants, although some of the endosomes labeled by PH(PLCδ)-GFP were grossly enlarged in *rme-1* mutants (Fig. S7 *J–K′*).

We also sought to confirm the results derived from imaging methods using biochemical methods. Thus, we measured PI(4,5)P2 levels in whole-animal lipid extracts, comparing *rab-10*, *cnt-1*, and *arf-6* mutants with wild-type controls, using thin-layer chromatography (TLC) followed by gas chromatography (30). To account for differences between samples in the efficiency of lipid extraction, we normalized the measured PI(4,5)P2 levels in the samples relative to the more abundant phospholipids phosphatidylcholine and phosphatidylinositol.

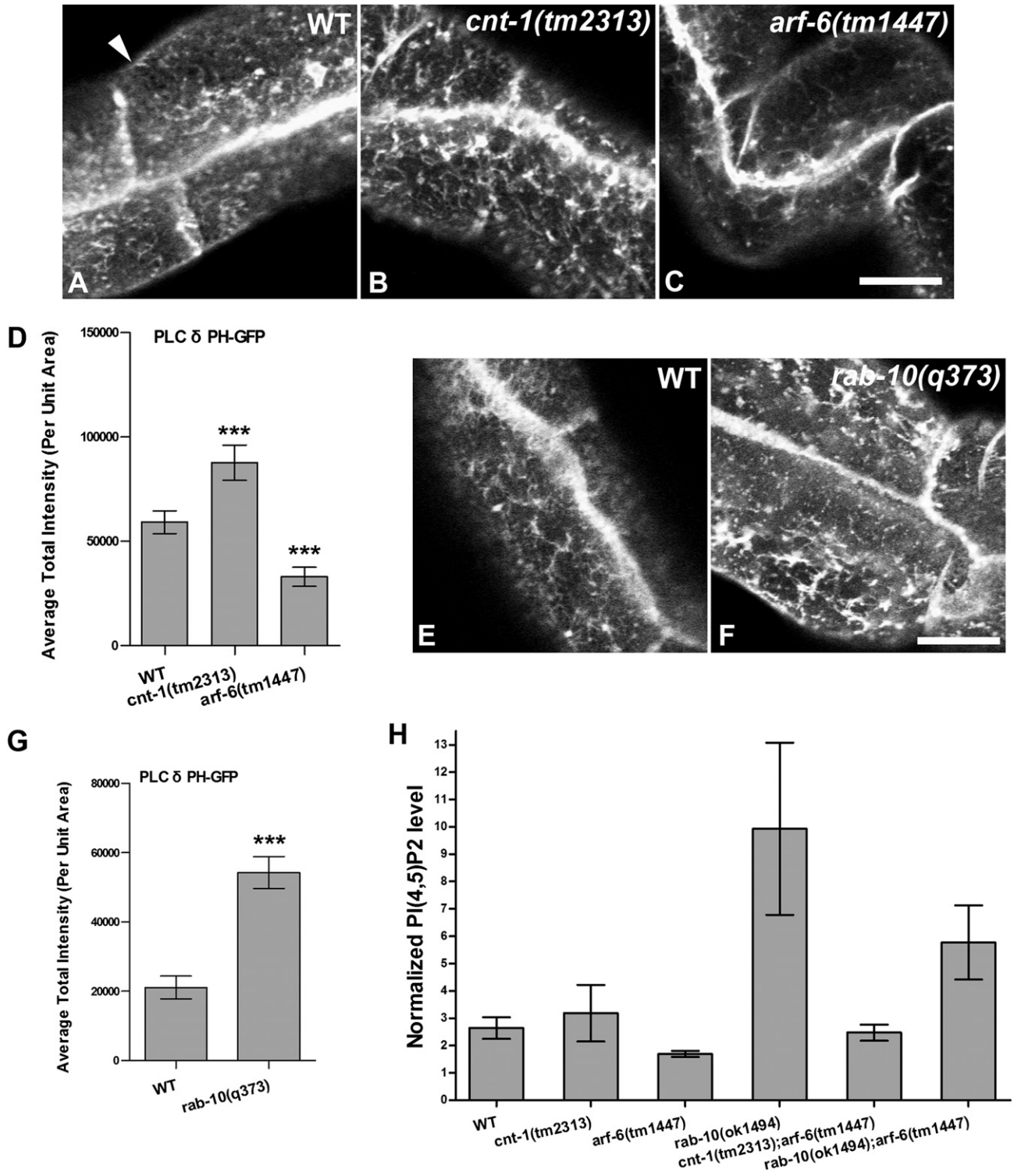

Fig. 4. (*A*–*G*) Endosomal accumulation of PH-GFP (PI(4,5)P2) was increased in *cnt-1(tm2313)* and *rab-10(q373)* mutants but was decreased in *arf-6(tm1447)* mutants. Representative confocal images are shown for PH-GFP in wild-type animals (*A* and *E*) and in *cnt-1(tm2313)* (*B*), *arf-6(tm1447)* (*C*), and *rab-10(q373)* (*F*) mutants. (Scale bar: 10 μm.) The arrowhead in *A* indicates basolateral membrane. (*D* and *G*) Quantification of average total intensity of PH-GFP per unit area. Error bars indicate SEM. $n = 18$; three different regions of the intestine (defined by a 100 × 100 pixel box positioned at random) were sampled in six animals of each genotype. ***$P < 0.001$, one-tailed Student's t test. (*H*) PI(4,5)P2 levels in *cnt-1(tm2313)*, *arf-6(tm1447)*, and *rab-10(q373)* mutants and in *cnt-1 (tm2313);arf-6(tm1447)*, *rab-10(q373);arf-6(tm1447)* double mutants. Whole-animal lipid extracts were prepared using TLC and were analyzed by gas chromatography. PI(4,5)P2 measurements were normalized to the abundant phospholipids (phosphatidylcholine and phosphatidylinositol) in each sample. Membrane PI(4,5)P2 levels are higher in *cnt-1* and *rab-10* mutants than in wild-type animals. Notably, consistent with the quantification of subcellular PH-GFP shown in *G*, the PI(4,5)P2 level is substantially higher in *rab-10* mutants than in wild-type animals. Conversely, the PI(4,5)P2 level is moderately decreased (35%) in *arf-6* mutants as compared with wild-type animals. The PI(4,5)P2 level appears fairly normal In *cnt-1(tm2313);arf-6(tm1447)* double mutants but is twofold higher in *rab-10(q373);arf-6(tm1447)* double mutants than in wild-type animals. The loss of ARF-6 reduces the elevated PI(4,5)P2 levels in *rab-10* mutants by about 40%. Data shown are the mean values and SEM from three independent experiments.

In agreement with the imaging data, our bulk lipid analysis detected elevated PI(4,5)P2 levels in *rab-10* mutants and reduced PI(4,5)P2 levels in *arf-6* mutants (Fig. 4*H*). Furthermore, we found that loss of ARF-6 reduced the elevated PI(4,5)P2 levels found in *rab-10* mutants by about 40%, further indicating that ARF-6 contributes to the effects of RAB-10 on PI(4,5)P2 (Fig. 4*H*). However, the bulk lipid analysis did not detect a clear difference in PI(4,5)P2 levels between wild-type animals and *cnt-1* mutants (Fig. 4*H*). This result may reflect a difference in the sensitivity of the two methods or the inability of the bulk lipid analysis approach to detect differences in specific phospholipid pools that can be detected using the imaging approach. For instance CNT-1 may affect only certain organelles (i.e., endosome versus plasma membrane pools) and/or tissues.

Endosomal Recruitment of Membrane-Bending Proteins Is Aberrant in *cnt-1* and *arf-6* Mutants. Changes in endosomal PI(4,5)P2 levels in *cnt-1* and *arf-6* mutants would be expected to affect the endosomal recruitment of endosomal PI(4,5)P2-binding proteins such as RME-1 and SDPN-1 (the *C. elegans* ortholog of Syndapin/Pacsin), endosomal proteins that are required for basolateral recycling in the intestine through their membrane-bending activities (10, 25). Consistent with this prediction, GFP-RME-1 and GFP-SDPN-1 endosomal labeling increased in *cnt-1* mutants and decreased in *arf-6* mutants (Fig. 5). Altered recruitment of these proteins, and others like them that participate in the recycling process, could explain the defects in recycling that we observed in *cnt-1* and *arf-6* mutants.

Clathrin and CNT-1 Coaccumulate on the Enlarged Endosomes of *arf-6* Mutants. ACAP1 has been reported to be part of a clathrin complex that functions on endosomes to promote the recycling of the insulin-responsive glucose transporter Glut4 and the adhesion molecule β-integrin (31). This work also indicated that endosomal clathrin accumulates when ACAP1 is overexpressed, but no previous studies have tested whether this effect on endosomal clathrin requires Arf6 (31). We found that CNT-1-GFP overaccumulates on endosomes in *arf-6* mutants (Fig. S4*B*). We further found that functional GFP-tagged clathrin heavy chain (GFP-CHC-1) showed a similar strong intracellular accumulation in *arf-6* mutants (Fig. S8*B*). Importantly, we noted that CNT-1-MC colocalizes with GFP-CHC-1 in wild-type animals (Fig. S8 *C–C″*) and that CNT-1-MC and GFP-CHC-1 coaccumulate on the enlarged endosomes of *arf-6*–null mutant animals (Fig. S8 *D–D″*). Although we do not yet understand the precise role of this pool of endosomal clathrin, our results do suggest that the endosomal clathrin could interact with CNT-1 and/or ARF-6 during endocytic sorting and recycling, although our data do not fit with a simple model in which ARF-6 acts to assemble endosomal clathrin.

Discussion

In this study, we further investigated the role of the RAB-10 GTPase in endocytic recycling, identifying an important link to endosomal PI(4,5)P2 regulation, in part through a newly identified interaction of RAB-10 with the ACAP homolog CNT-1. We defined the RAB-10–binding region within CNT-1 as the C-terminal ANK-repeat domain and provided evidence that RAB-10 is required for the endosomal recruitment of CNT-1. Our results suggest that RAB-10 is the dominant Rab recruiting CNT-1 to endosomes in the intestinal epithelium. Thus, CNT-1 is likely to provide a functional connection between members of different GTPase classes (RAB-10 and ARF-6) that are vital for endocytic recycling regulation. We went on to demonstrate misregulation of endosomal PI(4,5)P2 levels in *rab-10*, *cnt-1*, and *arf-6* mutants and showed that part of the effect of RAB-10 on PI(4,5)P2 depends upon ARF-6. Indeed, certain PI(4,5)P2-binding proteins of the recycling endosome that are implicated in membrane bending and membrane fission are recruited aberrantly upon the perturbation of any of these components. However, the effects of RAB-10 on endosomal PI(4,5)P2 were stronger than those of CNT-1, and not all the increased levels of PI(4,5)P2 detected in *rab-10* mutants could be suppressed by loss of ARF-6, indicating that RAB-10 also affects endosomal PI(4,5)P2 via additional mechanisms that remain to be identified. One possibility is that RAB-10 interacts with additional ARF regulators such as CNT-2. Alternatively RAB-10 may interact with additional effectors that control PI(4,5)P2 levels by a completely different mechanism.

RAB-10 appears to function at the interface of early endosomes and recycling endosomes, as reflected by its partial colocalization with early and recycling endosome markers and by the defects in morphology observed in both endosome types in *rab-10* mutants (5, 8). Given the importance of phosphoinositide species in determining distinct organelle identities, the control of endosomal PI(4,5)P2 by RAB-10 likely contributes to the biogenesis and/or maintenance of the basolateral recycling endosome compartment (1, 32). It remains unclear if such recycling endosomes form by the remodeling of early endosome fission products, which might be viewed as a maturation process. RAB-10 could act to promote the maturation of early endosomes to recycling endosomes or to define the identity of a particular subdomain within a complex, longer-lived recycling organelle.

Studies in mammals suggest that a complete Arf6 GTPase cycle (activation of Arf6 via GDP-to-GTP exchange and Arf6 inactivation through GTP-to-GDP hydrolysis) is necessary for functional transport, because the expression of GDP- or GTP-locked forms of Arf6 impairs cargo recycling, albeit at different steps in the transport process (13, 14). Our results, showing intracellular accumulation of hTAC-GFP in an *arf-6*–null mutant or under conditions predicted to cause overaccumulation of ARF-6(GTP), agree with this model. Loss of CNT-1 is expected to reduce GTP hydrolysis by ARF-6, leading to an increased level of active ARF-6-GTP, interfering with receptor recycling, as was observed with the expression of GTPase-defective Arf6. The overaccumulation of PI(4,5)P2 in *rab-10* and *cnt-1* mutants and the partial suppression of this defect in combination with *arf-6* mutants is consistent with the accumulation of abnormally high levels of ARF-6-GTP.

The RAB-10 effector CNT-1 also may contribute additional functions to the recycling process. CNT-1 harbors an N-terminal BAR domain. Proteins with BAR domains, such as amphiphysin, endophilins, and sorting nexins, have been reported to sense membrane curvature and to induce positive curvature, features that are important in membrane budding and tubulation (33). Recruited to the membrane by RAB-10, CNT-1 might be localized further to high-curvature regions of budding vesicles or tubules through its BAR domain or might help remodel functional subdomains or buds on endosomes, facilitating sequestration of recycling cargo.

Recent studies suggest that Rab-to-Arf signaling is an evolutionarily conserved process. Kanno et al. (34) recently identified binding of another recycling-associated Rab GTPase, Rab35, to ACAP2 in mammalian cells. That study also identified the ACAP2 ANK repeats as the Rab-binding domain for Rab35-mediated recruitment of ACAP2 to the plasma membrane. In mammalian macrophages it was demonstrated that Rab35, together with ACAP2, regulates phagocytosis (35). In addition, in PC12 cells, ACAP2 can be recruited by Rab35 to Arf6-positive endosomes, and ACAP2's Arf6-GAP activity is required for nerve growth factor-induced neurite outgrowth (36). None of these recent Rab35 studies directly assayed for effects on endosomal PI(4,5)P2 levels, effects on the recruitment of PI(4,5)P2-binding membrane–bending/fission proteins, or the requirement for Arf6 in these changes, but the reported defects could very well proceed via such mechanisms. Indeed, our studies also demonstrated that CNT-1 has the potential to interact with

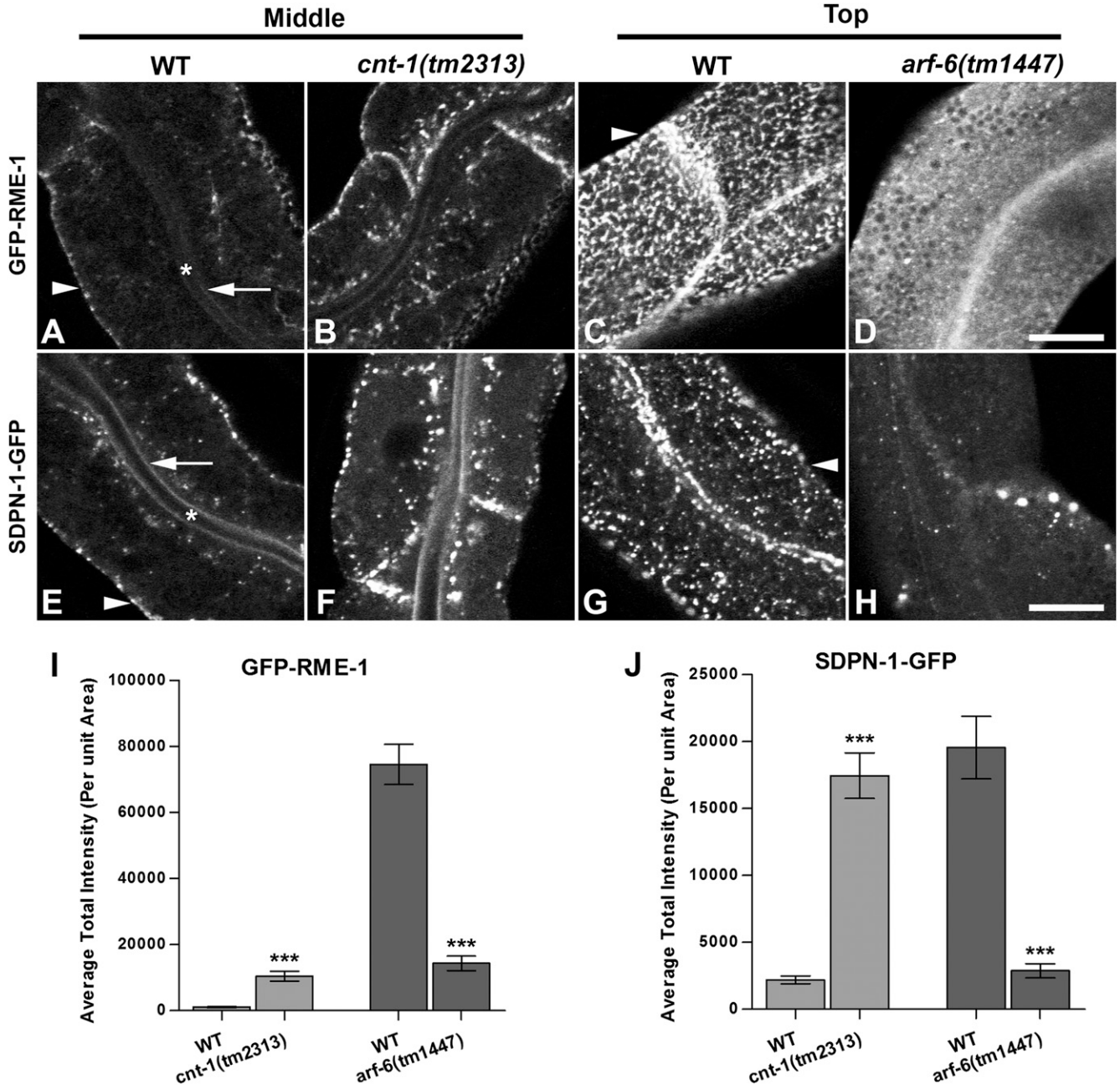

Fig. 5. Aberrant subcellular distribution of PI(4,5)P2-binding proteins GFP-RME-1 and GFP-SDPN-1 in *cnt-1* and *arf-6* mutants. (*A–D*) GFP-RME-1 medial endosomal labeling increased in *cnt-1* mutants, but its labeling of basolateral tubules and puncta decreased greatly in *arf-6* mutants. (*E–H*) Similar to GFP-RME-1, recycling endosome marker GFP-SDPN-1 medial labeling increased in *cnt-1* mutants, but labeling of basolateral tubules and puncta decreased greatly in *arf-6* mutants. Asterisks in *A* and *E* indicate intestinal lumen, arrows in *A* and *E* indicate apical membrane, and arrowheads in *A*, *C*, *E*, and *G* indicate basolateral membrane. (*I*) Quantification of GFP-RME-1 average total intensity per unit area. (*J*) Quantification of GFP-SDPN-1 average total intensity per unit area. Error bars indicate SEM. $n = 18$; three different regions of the intestine (defined by a 100 × 100 pixel box positioned at random) were sampled in six animals of each genotype. ***$P < 0.001$, one-tailed Student's t test. (Scale bar: 10 μm.)

RAB-35 in *C. elegans*. Although the RAB-35 interaction with CNT-1 did not appear physiologically important in the intestinal epithelium, both proteins are widely expressed and thus may interact functionally in another tissue or at another developmental time. Rab35 has been proposed to regulate PI(4,5)P2 at the intercellular bridge of cells during mitosis, but that regulation was proposed to be through interaction of Rab35 and the OCRL lipid phosphatase (37). It will be interesting to determine if a Rab35/ACAP/Arf6 cascade also contributes to the abscission process.

Rab/Arf functional interactions also can be reciprocal. In HeLa cells, Chesneau et al. (38) showed that Arf6-GTP can interact with Rab35 GAP EPI64B, negatively regulating Rab35 activity during cytokinesis. Together with our results, these observations provide compelling evidence that Rab-to-Arf and Arf-to-Rab regulatory loops represent a general mechanism for the coordinate regulation of Rabs and Arfs during membrane trafficking. Rab/Arf cross-talk is likely important for many higher-level processes that depend upon tight regulation of recycling endosome function.

Previous studies in mammals demonstrated a role for ACAP1 in Glut4 and integrin recycling (39, 40). Furthermore, ACAP1 was reported to be part of a clathrin-coat complex on endosomes (31). Although clathrin coats have been suggested to participate in the recycling process (41), the role of clathrin coats in endocytic recycling remains controversial. In our studies we found that GFP-CHC-1 colocalizes with CNT-1-MC on endosomes and that GFP-CHC-1 and CNT-1-MC coaccumulate on the enlarged endosomes of *arf-6* mutants, consistent with the idea of a conserved clathrin–ACAP interaction. However, the traditional role of an Arf protein is in recruiting clathrin adaptors, and thus loss of the Arf would be expected to reduce clathrin accumulation (42). Indeed, recent work indicated endosomal recruitment of the epithelial cell-specific clathrin adaptor complex AP-1B by Arf6 (43). Instead, we observed increased accumulation of endosomal clathrin in *arf-6*–null mutant *C. elegans*. Thus, our data do not fit with a simple model in which endosomal clathrin is recruited via ARF-6.

Although it has been suggested that the budding of clathrin-coated vesicles contributes to endocytic recycling, a flat clathrin lattice on endosomes has been suggested to create and/or maintain degradative subdomains on endosomes associated with HRS and ESCRT proteins, regulating the sorting of ubiquitinated cargo proteins in the endosome (44–46). Thus, another possibility is that ACAPs could interact with clathrin in the flat lattice to affect the balance in degradation and recycling that must be maintained in the endosomal system.

Materials and Methods

General Methods and Strains. All *C. elegans* strains were derived originally from the wild-type Bristol strain N2. Worm cultures, genetic crosses, and other *C. elegans* husbandry were performed according to standard protocols (47). Strains expressing transgenes were grown at 20 °C. A complete list of strains used in this study can be found in Table S1.

Antibodies. The mouse anti-HA monoclonal antibody (16B12) was purchased from Covance Research Products. The rabbit polyclonal antibody against *C. elegans* ARF-6 was produced against a peptide (CSTGDGLHEGLTWLSQN) corresponding to ARF-6 amino acids 157–172 coupled to keyhole limpet hemocyanin. The resulting serum was affinity purified using standard methods against the same peptide coupled to a HiTrap NHS-activated HP Column (GE Healthcare). The resulting purified antibodies were tested for specificity on Western blots of wild-type, *arf-6*–null, and ARF-6-GFP–expressing animals.

Yeast Two-Hybrid Analyses. The yeast two-hybrid screen for candidate RAB-10–interacting proteins was performed according to the procedure of the DupLEX-A yeast two-hybrid system (OriGene Technologies). The cDNA sequences of *C. elegans* rab-10(Q68L) in the entry vector pDONR221 were cloned into the pEG202-Gtwy bait vector by Gateway recombination cloning (Invitrogen) to generate N-terminal fusions with the LexA DNA-binding domain. pEG202-rab-5(Q78L), rab-7(Q68L), rab-8(Q67L), rab-10(+), rab-10 (T23N), rab-11(Q70L), and rab-35(Q69L) were constructed accordingly. The prenylation motifs for membrane attachment at the C-terminal ends of the Rabs were deleted to improve entry of bait fusion proteins into the yeast nucleus. The *C. elegans* DupLEX-A cDNA library was purchased from Origene Technologies.

The LexA-based DupLEX-A yeast two-hybrid system (OriGene Technologies Inc.) was used for all subsequent truncation analysis. All two-hybrid plasmids were generated as PCR products with Gateway attB.1 and attB.2 sequence extensions and were introduced into the Gateway entry vector pDONR221 by BP clonase II (Invitrogen) reaction. The bait vector pEG202-Gtwy and target vector pJG4-5-Gtwy have been described previously (7). Origene plasmid pSH18-34 (*URA3*, 8 ops.-LacZ) was used as reporter in all yeast two-hybrid experiments. Constructs were introduced into the yeast strain EGY48 (MATα trp1 his3 ura3 leu2::6 LexAop-*LEU2*) included in the system. Transformants were selected on plates lacking leucine, histidine, tryptophan, and uracil and containing 2% (wt/vol) galactose/1% (wt/vol) raffinose at 30 °C for 3 d and were assayed for the expression of the *LEU2* reporter. Blue/white β-galactosidase assays confirmed the results shown for growth assays, according to manufacturer's instructions.

Protein Expression and Coprecipitation Assays. *rab-5(Q78L), rab-7(Q68L), rab-8(Q67L), rab-10(Q68L),* and *rab-35(Q69L)* cDNA clones were transferred into an in-house modified vector pcDNA3.1 (+) (Invitrogen) with a 2xHA epitope tag and Gateway cassette (Invitrogen) for in vitro transcription/translation experiments. For GST pull-down experiments, equivalent *ehbp-1* (amino acids 662–901) and *cnt-1* (amino acids 656–826) PCR products were introduced in frame into vector pGEX-2T (GE Healthcare Life Sciences) modified with a Gateway cassette.

The N-terminally HA-tagged proteins RAB-5(Q78L), RAB7(Q68L), RAB-8 (Q67L), RAB-10(Q68L), and RAB-35(Q69L) were synthesized in vitro using the TNT-coupled transcription-translation system (Promega) using DNA templates pcDNA3.1-2xHA-RAB-5(Q78L), pcDNA3.1-2xHA-RAB-7(Q68L), pcDNA3.1-2xHA-RAB-8(Q67L), pcDNA3.1-2xHA-RAB10(Q68L), and pcDNA3.1-2xHA-RAB-35 (Q69L), respectively (1 μg/50 μL reaction). The reaction mixture was incubated at 30 °C for 90 min. Negative control GST was expressed in New England BioLabs Express *Iq*-competent *Escherichia coli* cells (New England BioLabs). GST-CNT-1 (amino acids 656–826) and GST-EHBP-1 (amino acids 662–901) fusion proteins were expressed in the *ArcticExpress* strain of *E. coli* (Stratagene). Bacterial pellets of GST and GST-EHBP-1(amino acids 662–901) were lysed in 20 mL B-PER Bacterial Protein Extraction Reagent (Pierce) with Complete Protease Inhibitor Mixture Tablets (Roche). Bacterial pellets of GST-CNT-1 (amino acids 656–826) were lysed using a EmulsiFlex-C3 homogenizer (Avestin) at 15,000 psi in 40 mL bacterial lysis buffer [50 mM Tris·HCL (pH 8.0), 20% (wt/vol) sucrose, 10% (wt/vol) glycerol, 2 mM DTT] with Complete Protease Inhibitor Mixture tablets (Roche). Extracts were cleared by centrifugation, and supernatants were incubated with glutathione-Sepharose 4B beads (Amersham Pharmacia) at 4 °C for 3 h. Beads then were washed six times with cold STET buffer [10 mM Tris·HCl (pH 8.0), 150 mM NaCl, 1 mM EDTA, 0.1% (vol/vol) Tween-20]. In vitro-synthesized HA-tagged protein (10 μL TNT mix diluted in 500 μL STET) was added to the beads and allowed to bind at 4 °C for 1 h. After six additional washes in STET, the proteins were eluted by boiling in 70 μL of 2× SDS/PAGE sample buffers. Eluted proteins were separated on SDS/PAGE [12% (wt/vol) polyacrylamide], blotted to nitrocellulose, and stained with Ponceau S to detect GST fusion proteins. After blocking, the blot was probed with anti-HA (16B12) antibody.

Plasmids and Transgenic Strains. To construct GFP or RFP/mCherry fusion transgenes for expression specifically in the worm intestine, a previously described *vha-6* promoter-driven vector modified with a Gateway cassette inserted at the Asp718I site just upstream of the GFP or RFP coding region was used. The sequences of *C. elegans cnt-1* cDNA (a gift from H. A. Baylis, University of Cambridge, Cambridge, UK) and *C. elegans arf-6* genomic DNA lacking a stop codon were cloned into entry vector pDONR221 by PCR and BP reaction and then were transferred into intestinal expression vectors by Gateway recombination cloning LR clonase II (Invitrogen) reaction to generate C-terminal fusions (5). Complete plasmid sequences are available on request. Low-copy integrated transgenic lines for all of these plasmids were obtained by the microparticle bombardment method (48).

Microscopy and Image Analysis. Live worms were mounted on 2% agarose pads with 10 mM levamisole as described previously (49). Multiwavelength fluorescence images were obtained using an Axiovert 200M microscope (Carl Zeiss Microimaging) equipped with a digital CCD camera (C4742–12ER; Hamamatsu Photonics), captured using Metamorph software version 6.3r2 (Universal Imaging), and then deconvolved using AutoDeblur Gold software version 9.3 (AutoQuant Imaging). Images taken in the DAPI channel were used to identify broad-spectrum intestinal autofluorescence caused by lipofuscin-positive lysosome-like organelles (50, 51). To obtain images of GFP fluorescence without interference from autofluorescence, we used argon 488-nm excitation and the spectral fingerprinting function of the Zeiss LSM510 Meta confocal microscope system (Carl Zeiss Microimaging) as described previously (5). Quantification of images was performed with Metamorph software version 6.3r2 (Universal Imaging). Most GFP/RFP colocalization experiments were performed on L3 and L4 larvae expressing GFP and RFP markers as previously described.

Whole-Animal Lipid Extracting, TLC, and Gas Chromatography. All *C. elegans* strains for lipid analysis were maintained at 20 °C using standard methods. For each strain animals were harvested from growth plates using M9 buffer, and worms were isolated by centrifugation. Pellets were ground in liquid N2 to a fine powder using mortar and pestle. Phospholipids were extracted under acidic conditions as described in König et al. (30). Phosphatidylinositol lipid standards were purchased from Avanti Polar Lipids. Phosphatidylcholine was purchased from MoBiTec.

ACKNOWLEDGMENTS. We thank Howard A. Baylis and Shohei Mitani for important reagents; Robin Chan and Gilbert DiPoalo for very helpful advice and discussions; and Peter Schweinsberg and Zui Pan for their generous advice and technical assistance. This work was supported by National Institutes of Health Grants GM067237 and 3R01GM067237-07S1 (to B.D.G.). R.B. was supported by a grant from the Aresty Research Center. S.E. was supported by the German Research Foundation Research Center for Molecular Physiology of the Brain.

1. Grant BD, Donaldson JG (2009) Pathways and mechanisms of endocytic recycling. *Nat Rev Mol Cell Biol* 10:597–608.
2. Donaldson JG (2005) Arfs, phosphoinositides and membrane traffic. *Biochem Soc Trans* 33:1276–1278.
3. Donaldson JG, Honda A (2005) Localization and function of Arf family GTPases. *Biochem Soc Trans* 33:639–642.
4. Linder MD, et al. (2007) Rab8-dependent recycling promotes endosomal cholesterol removal in normal and sphingolipidosis cells. *Mol Biol Cell* 18:47–56.
5. Chen CC, et al. (2006) RAB-10 is required for endocytic recycling in the Caenorhabditis elegans intestine. *Mol Biol Cell* 17:1286–1297.
6. Patino-Lopez G, et al. (2008) Rab35 and its GAP EPI64C in T cells regulate receptor recycling and immunological synapse formation. *J Biol Chem* 283:18323–18330.
7. Sato M, et al. (2008) Regulation of endocytic recycling by C. elegans Rab35 and its regulator RME-4, a coated-pit protein. *EMBO J* 27:1183–1196.
8. Shi A, et al. (2010) EHBP-1 functions with RAB-10 during endocytic recycling in Caenorhabditis elegans. *Mol Biol Cell* 21:2930–2943.
9. Glodowski DR, Chen CC, Schaefer H, Grant BD, Rongo C (2007) RAB-10 regulates glutamate receptor recycling in a cholesterol-dependent endocytosis pathway. *Mol Biol Cell* 18:4387–4396.
10. Pant S, et al. (2009) AMPH-1/Amphiphysin/Bin1 functions with RME-1/Ehd1 in endocytic recycling. *Nat Cell Biol* 11:1399–1410.
11. Babbey CM, et al. (2006) Rab10 regulates membrane transport through early endosomes of polarized Madin-Darby canine kidney cells. *Mol Biol Cell* 17:3156–3175.
12. Sano H, et al. (2007) Rab10, a target of the AS160 Rab GAP, is required for insulin-stimulated translocation of GLUT4 to the adipocyte plasma membrane. *Cell Metab* 5: 293–303.
13. D'Souza-Schorey C, et al. (1998) ARF6 targets recycling vesicles to the plasma membrane: Insights from an ultrastructural investigation. *J Cell Biol* 140:603–616.
14. Brown FD, Rozelle AL, Yin HL, Balla T, Donaldson JG (2001) Phosphatidylinositol 4,5-bisphosphate and Arf6-regulated membrane traffic. *J Cell Biol* 154:1007–1017.
15. Radhakrishna H, Donaldson JG (1997) ADP-ribosylation factor 6 regulates a novel plasma membrane recycling pathway. *J Cell Biol* 139:49–61.
16. Naslavsky N, Weigert R, Donaldson JG (2003) Convergence of non-clathrin- and clathrin-derived endosomes involves Arf6 inactivation and changes in phosphoinositides. *Mol Biol Cell* 14:417–431.
17. Eyster CA, et al. (2009) Discovery of new cargo proteins that enter cells through clathrin-independent endocytosis. *Traffic* 10:590–599.
18. D'Souza-Schorey C, Chavrier P (2006) ARF proteins: Roles in membrane traffic and beyond. *Nat Rev Mol Cell Biol* 7:347–358.
19. Honda A, et al. (1999) Phosphatidylinositol 4-phosphate 5-kinase alpha is a downstream effector of the small G protein ARF6 in membrane ruffle formation. *Cell* 99:521–532.
20. Yin HL, Janmey PA (2003) Phosphoinositide regulation of the actin cytoskeleton. *Annu Rev Physiol* 65:761–789.
21. Inoue H, Randazzo PA (2007) Arf GAPs and their interacting proteins. *Traffic* 8: 1465–1475.
22. Jackson TR, et al. (2000) ACAPs are arf6 GTPase-activating proteins that function in the cell periphery. *J Cell Biol* 151:627–638.
23. Shinozaki-Narikawa N, Kodama T, Shibasaki Y (2006) Cooperation of phosphoinositides and BAR domain proteins in endosomal tubulation. *Traffic* 7:1539–1550.
24. Kouranti I, Sachse M, Arouche N, Goud B, Echard A (2006) Rab35 regulates an endocytic recycling pathway essential for the terminal steps of cytokinesis. *Curr Biol* 16:1719–1725.
25. Shi A, et al. (2007) A novel requirement for C. elegans Alix/ALX-1 in RME-1-mediated membrane transport. *Curr Biol* 17:1913–1924.
26. Sato T, et al. (2007) The Rab8 GTPase regulates apical protein localization in intestinal cells. *Nature* 448:366–369.
27. Brown PS, et al. (2000) Definition of distinct compartments in polarized Madin-Darby canine kidney (MDCK) cells for membrane-volume sorting, polarized sorting and apical recycling. *Traffic* 1:124–140.
28. Stenmark H (2009) Rab GTPases as coordinators of vesicle traffic. *Nat Rev Mol Cell Biol* 10:513–525.
29. Garcia P, et al. (1995) The pleckstrin homology domain of phospholipase C-delta 1 binds with high affinity to phosphatidylinositol 4,5-bisphosphate in bilayer membranes. *Biochemistry* 34:16228–16234.
30. König S, Hoffmann M, Mosblech A, Heilmann I (2008) Determination of content and fatty acid composition of unlabeled phosphoinositide species by thin-layer chromatography and gas chromatography. *Anal Biochem* 378:197–201.
31. Li J, et al. (2007) An ACAP1-containing clathrin coat complex for endocytic recycling. *J Cell Biol* 178:453–464.
32. Di Paolo G, De Camilli P (2006) Phosphoinositides in cell regulation and membrane dynamics. *Nature* 443:651–657.
33. Casal E, et al. (2006) The crystal structure of the BAR domain from human Bin1/amphiphysin II and its implications for molecular recognition. *Biochemistry* 45: 12917–12928.
34. Kanno E, et al. (2010) Comprehensive screening for novel Rab-binding proteins by GST pull-down assay using 60 different mammalian Rabs. *Traffic (Copenhagen, Denmark)*11:491–507.
35. Egami Y, Fukuda M, Araki N (2011) Rab35 regulates phagosome formation through recruitment of ACAP2 in macrophages during FcγR-mediated phagocytosis. *J Cell Sci* 124:3557–3567.
36. Kobayashi H, Fukuda M (2012) Rab35 regulates Arf6 activity through centaurin-β2 (ACAP2) during neurite outgrowth. *J Cell Sci* 125:2235–2243.
37. Dambournet D, et al. (2011) Rab35 GTPase and OCRL phosphatase remodel lipids and F-actin for successful cytokinesis. *Nat Cell Biol* 13:981–988.
38. Chesneau L, et al. (2012) An ARF6/Rab35 GTPase cascade for endocytic recycling and successful cytokinesis. *Curr Biol* 22:147–153.
39. Dai J, et al. (2004) ACAP1 promotes endocytic recycling by recognizing recycling sorting signals. *Dev Cell* 7:771–776.
40. Li J, et al. (2005) Phosphorylation of ACAP1 by Akt regulates the stimulation-dependent recycling of integrin beta1 to control cell migration. *Dev Cell* 9:663–673.
41. van Dam EM, Stoorvogel W (2002) Dynamin-dependent transferrin receptor recycling by endosome-derived clathrin-coated vesicles. *Mol Biol Cell* 13:169–182.
42. Krauss M, et al. (2003) ARF6 stimulates clathrin/AP-2 recruitment to synaptic membranes by activating phosphatidylinositol phosphate kinase type Igamma. *J Cell Biol* 162:113–124.
43. Shteyn E, Pigati L, Fölsch H (2011) Arf6 regulates AP-1B-dependent sorting in polarized epithelial cells. *J Cell Biol* 194:873–887.
44. Raiborg C, Bache KG, Mehlum A, Stang E, Stenmark H (2001) Hrs recruits clathrin to early endosomes. *EMBO J* 20:5008–5021.
45. Raiborg C, Wesche J, Malerød L, Stenmark H (2006) Flat clathrin coats on endosomes mediate degradative protein sorting by scaffolding Hrs in dynamic microdomains. *J Cell Sci* 119:2414–2424.
46. Shi A, et al. (2009) Regulation of endosomal clathrin and retromer-mediated endosome to Golgi retrograde transport by the J-domain protein RME-8. *EMBO J* 28:3290–3302.
47. Brenner S (1974) The genetics of Caenorhabditis elegans. *Genetics* 77:71–94.
48. Praitis V, Casey E, Collar D, Austin J (2001) Creation of low-copy integrated transgenic lines in Caenorhabditis elegans. *Genetics* 157:1217–1226.
49. Sato M, et al. (2005) Caenorhabditis elegans RME-6 is a novel regulator of RAB-5 at the clathrin-coated pit. *Nat Cell Biol* 7:559–569.
50. Clokey GV, Jacobson LA (1986) The autofluorescent "lipofuscin granules" in the intestinal cells of Caenorhabditis elegans are secondary lysosomes. *Mech Ageing Dev* 35:79–94.
51. Hermann GJ, et al. (2005) Genetic analysis of lysosomal trafficking in Caenorhabditis elegans. *Mol Biol Cell* 16:3273–3288.